Characterization of Eyjafjallajökull volcanic ash particles and a protocol for rapid risk assessment

S. R. Gislason[a], T. Hassenkam[b], S. Nedel[b], N. Bovet[b], E. S. Eiriksdottir[a], H. A. Alfredsson[a], C. P. Hem[b], Z. I. Balogh[b], K. Dideriksen[b], N. Oskarsson[a], B. Sigfusson[c], G. Larsen[a], and S. L. S. Stipp[b,1]

[a]Institute of Earth Sciences, University of Iceland, Sturlugata 7, 101 Reykjavik, Iceland; [b]Nano-Science Center, Department of Chemistry, University of Copenhagen, 2100 Copenhagen, Denmark; and [c]Reykjavik Energy, Baejarhalsi 1, 110 Reykjavik, Iceland

Edited* by Robert A. Berner, Yale University, New Haven, CT, and approved March 15, 2011 (received for review October 24, 2010)

On April 14, 2010, when meltwaters from the Eyjafjallajökull glacier mixed with hot magma, an explosive eruption sent unusually fine-grained ash into the jet stream. It quickly dispersed over Europe. Previous airplane encounters with ash resulted in sandblasted windows and particles melted inside jet engines, causing them to fail. Therefore, air traffic was grounded for several days. Concerns also arose about health risks from fallout, because ash can transport acids as well as toxic compounds, such as fluoride, aluminum, and arsenic. Studies on ash are usually made on material collected far from the source, where it could have mixed with other atmospheric particles, or after exposure to water as rain or fog, which would alter surface composition. For this study, a unique set of dry ash samples was collected immediately after the explosive event and compared with fresh ash from a later, more typical eruption. Using nanotechniques, custom-designed for studying natural materials, we explored the physical and chemical nature of the ash to determine if fears about health and safety were justified and we developed a protocol that will serve for assessing risks during a future event. On single particles, we identified the composition of nanometer scale salt coatings and measured the mass of adsorbed salts with picogram resolution. The particles of explosive ash that reached Europe in the jet stream were especially sharp and abrasive over their entire size range, from submillimeter to tens of nanometers. Edges remained sharp even after a couple of weeks of abrasion in stirred water suspensions.

Iceland volcano | European airspace | grain size distribution | atomic force microscopy | X-ray photoelectron spectroscopy

The recent volcanic activity in south Iceland, that began late evening on March 20, 2010, had been preceded for some weeks by intense seismic activity and deformation (1). Lava flowed from a fissure on the ice-free flank of the Eyjafjallajökull volcano, but ashfall from its 1-km high plume was insignificant. After a hiatus of about a couple of days, during which earthquakes signaled rising magma, eruption recommenced early morning, April 14, this time from within the caldera, under 200–300 m of ice. Jökulhlaups, floods of meltwater, flowed down the northern and southern slopes and reached the lowlands around noon. Roads, infrastructure, and farmlands were destroyed but people had been evacuated so there was no loss of life. This second phase was explosive, sending exceptionally fine-grained ash almost 10 km through the troposphere, into the stratosphere (1).

Animals were kept inside or evacuated as plumes blackened the Icelandic sky. From April 15, when the very fine ash blew east and south, airspace closed over most of Europe. Effusion rate was maximum during the first 3 d. The ash was gray, trachyandesitic, with 58 mass % silica (Table S1). After April 18, ash production decreased by 1–2 orders of magnitude. Composition was essentially the same, 57% SiO_2, but the ash took on a more typical character, namely larger particles, black and glassy. During May, a few forceful explosions projected ash to the jet stream and before activity decreased on May 23, lava reached halfway to the glacial outwash plain. The plumes that caused the 7 d air traffic disruption resulted directly from the explosive nature of the ash, caused by the interaction of magma and water. By about April 20, water flow into the crater and fine ash production had ceased, and air traffic returned to normal. Reuters reported losses estimated between 1.5 and 2.5 billion € and 10 million travelers were affected.

Fears about danger to aircraft arose from an incident when a British Airways 747 flew through an ash cloud during the 1982 eruption of Mount Galunggung in Indonesia. The pilot reported sparks from the windows and wings as ash sandblasted all surfaces and all four jet engines failed when melted ash coated their interior (2). Luckily for the 263 passengers and crew, the pilot could restart three of the engines after they cooled during descent and he landed while peeking through a strip a couple of inches wide on the side window that had avoided sandblasting. This event provided powerful motivation for the international aviation community.

Ash ingestion and inhalation were also concerns in Iceland and across Europe. Airborne particles and toxic gases (e.g., SO_2, HF) pose respiratory hazards (3, 4). Particles < 10 nm diameter cause irritation on the short term and cancer on the long term. Silicosis is a chronic, often fatal, condition caused by micro- and nanoscale particles (3, 5). Health risk from the physical nature of the particles is augmented by condensed salts, acids, and trace elements and these also threaten surface waters and terrestrial ecosystems (6–10). In Iceland, extensive public education and assistance minimized danger for people and animals. Across Europe, there were discussions about the consequence of ash fallout on health and on climate.

Such extensive airspace closure, completely unprecedented, had a huge economic impact and caused irritation and hardship for passengers, their families, and businesses. The general population felt insecure about health risks. Was it dangerous to inhale the ash particles? Should nursery schools be closed? Were water supplies at risk? Had correct decisions been made about airport closures? Considering the economic costs, will correct decisions be made in the future? In general, authorities needed better information about the ash and its effects, but scientific literature was unavailable and accepted protocols for characterizing the ash for making decisions were simply nonexistent.

The purpose of this paper is to provide information about the Eyjafjallajökull ash, from the physical and chemical perspectives, and to suggest a protocol consisting of several rapid and

Author contributions: S.L.S.S. planned the project; S.R.G. and H.A.A. collected the samples; S.R.G. and S.L.S.S. organized the research; T.H, S.N. and N.B. developed methods; S.R.G., T.H., S.N., N.B., E.S.E., H.A.A., C.P.H., Z.I.B., K.D., N.O., B.S., G.L., and S.L.S.S. performed research; S.R.G., T.H., S.N., N.B., E.S.E., H.A.A., C.P.H., Z.I.B., K.D., N.O., B.S., G.L., and S.L.S.S. intepreted data; and S.L.S.S. wrote the paper.

The authors declare no conflict of interest.

*This Direct Submission article had a prearranged editor.

[1]To whom correspondence should be addressed. E-mail: stipp@nano.ku.dk.

This article contains supporting information online at www.pnas.org/lookup/suppl/doi:10.1073/pnas.1015053108/-/DCSupplemental.

straightforward analyses that can provide data for judging risks for aircraft operations and health in the future. To develop this protocol, we have gathered information from the methods traditionally used to investigate tephra (volcanic ash) and combined it with observations from nanotechniques. We report on the size, shape, and hardness (i.e., the ability of the nanoparticles to put airplanes at risk) as well as the chemical composition of the salt condensates on the particle surfaces (i.e., the toxic nature of the nanoparticles). We used ash that was absolutely fresh and analyzed immediately, and then after exposure to pure water and nitric acid, as models for behavior during exposure to rain, fog, and volcanic emissions. We compared two samples, one collected April 15, 2010, immediately after the explosive eruption began, and another collected April 27, after glacier water inflow into the crater had ceased. Both samples were collected and maintained dry. Most previous studies have examined samples weeks or years after eruption, or fresh samples but after exposure to rain or fog (11).

Physical Aspects of the Eyjafjallajökull Ash

The early ash from the hydromagmatic, explosive phase (termed here explosive ash, but often referred to as phreato-magmatic ash) was surprisingly soft, light, and powdery. It fell absolutely silently. In the sample bag, the particles were cohesive, the consistency of flour. The later, magmatic ash was more typical (called typical ash); it was granular with the consistency of dry sand and particles could be heard falling on hard surfaces. BET (Brunauer, Emmett, Teller, ref. 12) surface area analysis confirmed the differences. The explosive ash was 4.3 m^2/g; the typical ash was 0.45 m^2/g. Electron microprobe (EMPA) backscattered images (Fig. 1*A*), scanning electron microscopy (SEM), and X-ray tomography (XT) showed that explosive ash particles range in diameter from approximately 300 μm to a few tens of nanometers, whereas the typical ash completely lacks the small diameter fraction (Fig. 1*B*). The explosive ash was also remarkable in its abundance of tiny particles attached to larger grains (Figs. 2*A* and 3*A*). Even after extensive abrasion in water (solid : liquid = 1 : 1,000), much of this very fine material remained (Figs. 2*B* and 3*B*) and some grains were still entirely composed of aggregated nanoparticles (Fig. 2*C*). Atomic force spectroscopy (AFS) explains why; the surfaces are particularly adhesive (Fig. 2 *D–F*).

The explosive ash was bimodal in size distribution with peaks at about 25- and 200-μm diameter (Fig. 1*C*; >250 μm, dry sieving; <250 μm, laser absorption from dry air suspension). For the typical ash, diameter peaked at approximately 500 μm. At least 20 mass % of the explosive ash was <10 μm, the inhalation risk limit. SEM and atomic force microscopy (AFM) demonstrate that particle size analysis underestimates the total <10-μm fraction because the resolution limit is approximately 1.8 μm, and a significant portion of nanoparticles adhere on or aggregate as larger particles. For more typical ash, the <10-μm fraction is <2 mass %, with much smaller surface area, consistent with previous studies of Icelandic ash that had not reacted to form secondary minerals (13) and samples collected from other sites. Explosive volcanic ash particles, smaller than 100 μm and not containing hydrothermal phases, from five volcanoes (posteruption age from 6 to 37 y) had surface area of 1–2 m^2/g (14), which is the same range as for three samples from another study (20 and 30 y and 11 My old; ref. 15). Only 10% of the ash from Mount Saint Helens was <10 μm but 13–20% of ash from Soufrière Hills, Monserat was in the dangerous range, with considerable cristobalite (16). Submicrometer scale quartz is more dangerous than generic volcanic ash and cristobalite is twice as hazardous as quartz (16). In the Eyjafjallajökull ash, there was very little quartz, and cristobalite was not detected.

The exceptionally fine nature of the early ash was a direct result of its explosive origin. Glacial meltwater chilled the magma, promoting strain disintegration. Shock waves from steam explosions caused mechanical fragmentation and oxidation by steam increased magma liquidus temperature, causing expulsion of dissolved volatiles during cooling, further fracturing the particles. On the ground beneath the plume center, airborne material was so dense that sunlight was blocked; here, particles were smallest, linking explosiveness with grain size. The extremely fine nature and the explosive ejection to the stratosphere led directly to long-range transport. In a dispersing plume, particles <63-μm diameter can remain suspended for days (17, 18), allowing ash to reach Russia and the Mediterranean.

EMPA (Fig. 1*A*) and SEM (Figs. 2 *A–C* and 3 *A* and *B*) show the asperity of the explosive ash. Even the nanoparticles are far from round. Their sharpness makes them particularly abrasive. We tested if exposure to water, such as rain or fog, could round them by stirring them vigorously in water for a couple of weeks. They remained sharp. Sandblasting studies prove that shape is an important factor in abrasion, even more important than mass. The speed with which an airplane would interact with a plume of very fine-grained ash would ensure that even nanoparticles would have the necessary momentum to wear surfaces, especially particles that are sharp and hard.

The hardness of a particle is determined by its composition and crystal structure. EMPA and X-ray diffraction (XRD) demonstrated that Eyjafjallajökull ash is dominated by andesitic glass, which has Mohs scale hardness of about 5.5–6, and crystals of

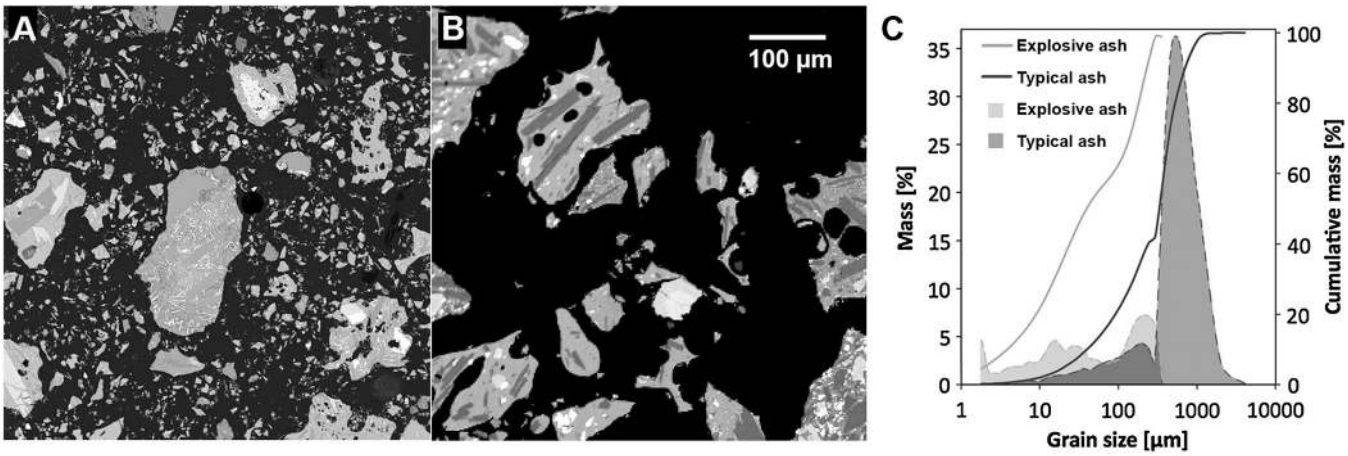

Fig. 1. Particle size and shape (EMPA backscattered electron images; both same scale) for (*A*) the explosive ash, (*B*) typical ash, and (*C*) particle size distribution. The explosive ash particles are sharp, even at nanometer scale.

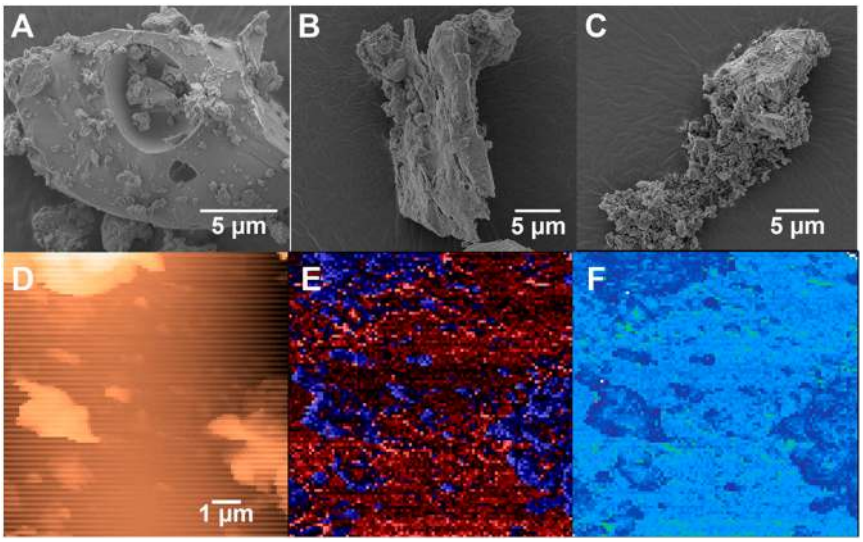

Fig. 2. (*A–C*) SEM images of (*A*) fresh explosive ash; edges are sharp, even on the adhering nanoparticles; (*B*) after stirring in pure water for 90 min; edges are still sharp and particles still adhere; (*C*) nanoparticles remain aggregated even after stirring, suggesting they are sintered. (*D–F*) AFS maps of the surface of one particle, such as that shown in *A*, constructed from data from 10,000 force/distance curves, collected using a standard silicon tip; (*D*) image representing topography from maximum force data (dark marks the smooth particle surface) with adhering nanoparticles (closer to the observer, lighter color); (*E*) the same area constructed with adhesion force data; the large particle surface (pink to red) is most adhesive, black represents the middle adhesion range, and the adhering particles (blue) are not sticky; (*F*) the same area showing elasticity; the surface (green to pale blue) is most elastic and the particles (dark blue) are rigid. Hassenkam et al. (37) explain AFS in more detail.

plagioclase, pyroxene, and olivine, with hardness of 6, 7, and 6.5. The ash particles are much harder than the exposed parts on an airplane: glass windows, aluminum, epoxy, and paint. Indeed, paint is usually removed from airplanes by jets of wheat starch or polyacrylate to avoid damage. Clearly ash particles are harder and sharper—enough to turn a pilot's window opaque. The Eyjafjallajökull glass softens at approximately 890 °C and melting is complete at 1,147 °C. Pyroxene melts at approximately 1,100 °C, plagioclase at around 1,200 °C, and olivine at about 1,400 °C (19). Thus, the ash would easily melt in a jet engine, which reaches temperatures of 1,500–2,000 °C (20, 21). The smaller the particles, the more easily they melt, creating fine droplets that condense on cooler engine parts.

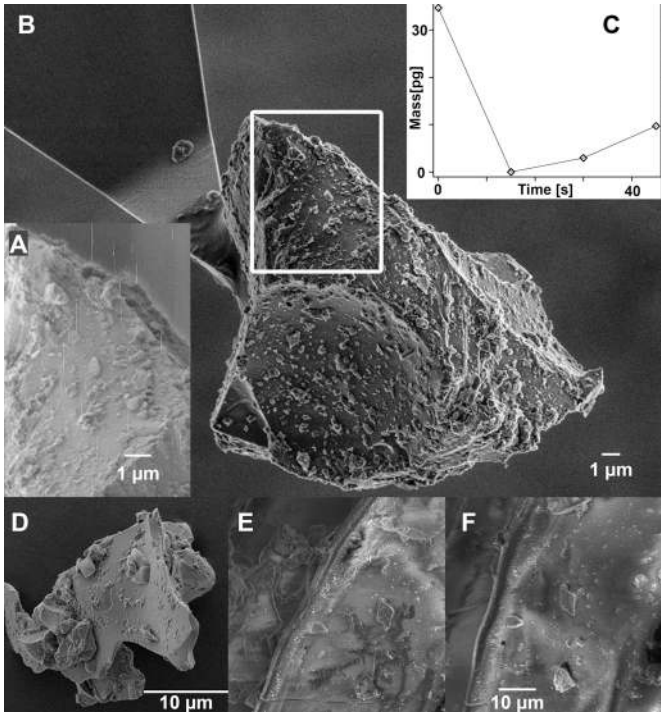

Fig. 3. An explosive ash particle glued to an AFM cantilever (*A*) fresh and (*B*) after exposure to water for a total of 45 s; particles remain attached while (*C*) salt is lost. The tiny mass gain (approximately 4 pg) results when the epoxy absorbs water. SEM images of (*D*) a fresh, typical ash particle with layers and rounded salt condensates; (*E*) the surface of another particle before, and (*F*) the same site after exposure to water; material has been removed on the terraces above and below the step edge. A slightly different angle of view for *E* and *F* produces slight distortion.

Surface Composition of the Eyjafjallajökull Ash

The bulk composition for the explosive and typical ash was the same (Table S1), but their surface composition was vastly different (Table 1). X-ray photoelectron spectroscopy (XPS), which collects information from the top 10 nanometers of a solid, shows that surface salts, clearly present initially, dissolve in distilled water and dilute HNO_3. Knowing surface composition makes it possible to estimate which salts condensed from the volcanic gases, which has not previously been possible. Indeed, Witham et al. (22) stated in their review that volatile condensation processes are not well understood.

The relative concentration (element %) of surface salts, particularly Cl and F, is lower on the explosive ash (Table 1) because the volume of volatiles available for condensation was lower during the initial eruptions. Instead of being ejected into the plume, the volatiles were dissolved in the meltwater and transported away as solutes. Total dissolved concentrations for F, Al, Fe, Mn and Br in the floodwaters on April 14 were high, well above EU drinking water standards. After exposure to water, the typical ash had higher surface concentration of Si and O, elements indicative of the bulk; removal of surface condensates brought the bulk particle into XPS range. In contrast, composition change after rinsing the explosive ash was minimal, consistent with a much thinner layer of surface salts. Treatment with 10^{-3} M HNO_3 further removes surface material, particularly F. The increase in surface C, called adventitious carbon, results from hydrocarbon contamination that comes from air or solution and is normal for samples exposed to ambient conditions (23).

Table 1. Bulk composition (italics text) compared with surface composition (normal text) on fresh and solution exposed samples, all expressed as relative element % (more explanation at the bottom of the table)

	Explosive ash			Typical ash		
	Fresh-surface (*bulk*)	90 min; pure water	90 min; 10^{-3} M HNO_3	Fresh-surface (*bulk*)	90 min; pure water	90 min; 10^{-3} M HNO_3
O	56.2 (*45.4*)	56.3	58.2	43.0 (*45.1*)	55.2	57
Si	25.5 (*27.1*)	25.6	26.6	23.8 (*26.5*)	30.7	33.6
Al	7.0 (*7.87*)	7.0	5.1	4.0 (*7.75*)	1.6	1.5
Fe	2.6 (*7.58*)	2.5	2.3	3.1 (*7.72*)	4.3	1.7
Mg	2.5 (*1.39*)	1.8	1.4	1.4 (*1.90*)	0.4	0.5
Na	1.8 (*3.72*)	1.2	0.7	0.9 (*3.74*)	0.1	0.1
Ca	1.2 (*3.93*)	1.5	0.8	2.0 (*4.37*)	0.4	0.6
C	1.1	2.7	4.4	4.3	5.3	3.6
K	0.8 (*1.49*)	0.8	0.2	0.4 (*1.36*)	0	0
Cl	0.4	0	0	9.5	0.3	0
F	0.4	0.3	0	6.9	1.1	0.6
Ti	0.3 (*1.08*)	0.3	0.3	0.4 (*1.13*)	0.6	0.3
P	0.2 (*0.23*)	0	0	0.3 (*0.19*)	0	0.5
ratio						
Al/Si	0.028	0.273	0.192	0.168	0.052	0.045
Fe/Si	0.102	0.098	0.086	0.13	0.14	0.051
Mg/Si	0.098	0.07	0.053	0.059	0.013	0.015
Na/Si	0.071	0.047	0.026	0.038	0.003	0.003
Ca/Si	0.047	0.059	0.03	0.084	0.013	0.018
K/Si	0.031	0.031	0.008	0.017	0	0
Cl/Si	0.016	0	0	0.399	0.02	0
F/Si	0.016	0.012	0	0.29	0.036	0.018
Ti/Si	0.012	0.012	0.011	0.017	0.02	0.009
P/Si	0.008	0	0	0.013	0	0.015

Composition of the bulk ash samples was derived using ICP-OES (inductively coupled plasma optical emission spectroscopy). The full dataset is presented in Table S1. XPS (X-ray photoelectron spectroscopy) analyses the surface, only the top 10 nm, so as surface salt coatings are dissolved away, more of the bulk composition is recorded in the analyses. We used a monochromated $Al_{K\alpha}$ source; chamber pressure was always $<5 \times 10^{-9}$ atm; all samples were analyzed with the same instrument parameters and beam time.

In water–ash mixtures, pH remained relatively constant (Table S2); it was slightly basic for the explosive ash (pH ~ 8), typical of waters at equilibrium with basalt, suggesting negligible acidic gas condensate. Protons from solution exchange rapidly with surface cations of glass and minerals (24), but if proton salts are abundant, pH is low, as was reported for Mount Hekla ash (25) and as we observed for the typical ash (pH ~ 5).

SEM images of glassy particles from the typical ash show layers and rounded nanoparticles (Fig. 3*D*) that disappear after exposure to solution. Layers of salts (Fig. 3*E*) are eroded as water dissolves them (Fig. 3*F*). Even on the surfaces of the explosive ash, submicrometer scale AFM imaging shows smooth, flat salt layers (Fig. 4*A*) that dissolved during exposure to water for 24 h and small, secondary minerals formed (Fig. 4*B*). Geochemical speciation modeling of the leachates (PHREEQC; ref. 26) suggests these features to be Fe(III) oxides, probably goethite, which forms from Fe(II) released from the ash in contact with oxygen.

In leachate experiments, typical ash surfaces give up Ca, Al, and Fe(II) and if pH is high, CO_2 enters from air (Table S2). The water : ash ratio was high (597–1,006) to minimize secondary mineral formation. Surface salts dissolve rapidly, after <15 min (Table S2). Salt release rate, estimated from Cl, SO_4, and F concentrations, was approximately $10^{-6.3}$, 10^{-7}, and $10^{-7.6}$ mol/m^2 s, several orders of magnitude lower than expected for pure halite, gypsum, or fluorite (27, 28), confirming the presence of these elements in other, less soluble minerals. Release rate was faster than for glass and olivine (29, 30), even considering enhancement

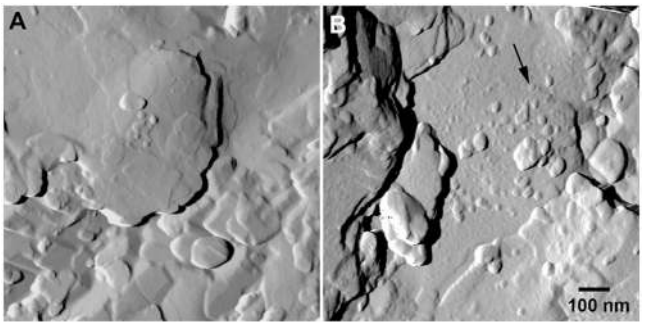

Fig. 4. AFM images of the surface of an explosive ash particle (*A*) fresh and (*B*) after exposure to water for 24 h. Smooth, flat, salt layers were removed and a secondary phase nucleated (such as at arrow), probably goethite.

by F (31). Combining information from surface composition, speciation modeling, and known volcanic fumarole incrustation and evaporite minerals (32, 33) provides estimates of the surface condensates (Table S3). We can also use the data to estimate average thickness of salt layers: approximately 0.6 nm for the explosive ash and approximately 4 nm for the typical ash. Calculations confirmed undersaturation in the leachates for all common volcanic salts, primary minerals, and glasses. All data are consistent with the presence of epsomite, $MgSO_4 \cdot 7H_2O$; scacchite, $MnCl_2$; melanterite, $FeSO_4 \cdot 7H_2O$; Na-metaborate, $NaBO_2$; Na-orthophosphate, Na_3PO_4; ralstonite, $NaMgAlF_4(OH)_2 \cdot (H_2O)$; hieratite, K_2SiF_6; malladrite, Na_2SiF_6; thenardite, $Na_2SO_4 \cdot 10H_2O$; arkanite, K_2SO_4; halite, NaCl; and antarcite, $CaCl_2 \cdot 6H_2O$ (Table S3).

An interesting question is how much mass is available for release from the salts of an ash plume, if they are rinsed away by rain or if the ash falls into lakes, rivers, or the ocean. It is not possible to determine the difference in mass before and after exposure to water, because the change is smaller than the error introduced by loss during filtration or centrifugation. A simple estimate from the bulk dissolved concentration data (Tables S2 and S3) gives an overall average (0.5% and 0.2% for the explosive and typical ash), but it is not possible to know if the solution data represent salts rinsed from the surface, from dissolution of the ash itself, from precipitation of secondary minerals, or from some combination. Instead, we developed a method that provides mass loss directly from a single particle, within tens of seconds, at picogram (pg; 10^{-12} g) resolution.

Fig. 3 shows an AFM cantilever, to which a single particle of explosive ash had been glued. Oscillation of the cantilever before and after particle mounting provides total, initial particle mass. The particle-glue-cantilever assembly was exposed to 3 mL of pure water for 15 s, then dried and oscillated again. Each rinse was made in a fresh water aliquot to minimize secondary mineral precipitation and each rinse-dry-oscillate cycle gave one datum on Fig. 3*C*. After only a few seconds, the salts were released. Mass loss was 35 pg, 0.4% of the total initial mass, which corresponds to about 10–20-nm thickness (assuming a salt density of about 2.7 g/cm^3). Typical ash particles (such as Fig. 5*D*) are so extensively covered with salts that, in five experiments, the epoxy could never make contact with the particle, so after 10 s exposure to water, salt dissolved and the particles detached. Sometimes salt remnants could be seen on the cantilever. One such remnant (Fig. 5*B*) weighed approximately 6 pg, and dissolved in little over a minute at a rate of approximately 40 femtograms per second (fg/s; 10^{-15} g/s). The fragment, which probably does not represent the full salt thickness, was about 300-nm thick.

Volcanic gases that condense on ash particles reach the ground sooner than if they remain airborne, but not all volatiles adsorb to the same degree or at the same temperature, so the concentrations measured in leachates do not represent volatile composition and can be misleading if the volcanic gases react with the ash.

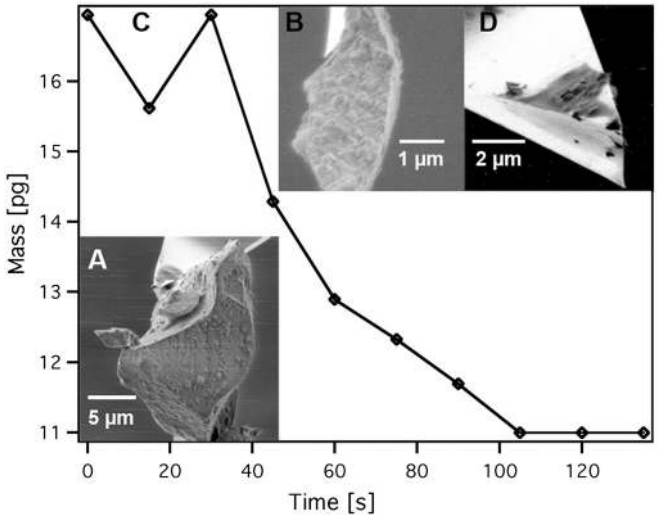

Fig. 5. SEM image of (*A*) a fresh particle of typical ash glued to an AFM tip with epoxy; salt layers and rounded condensates are visible. After exposure to water, salt dissolved and the particle fell from the cantilever, leaving (*B*) a small fragment of salt behind; its mass was approximately 6 pg. (*C*) After 100 s in water, the salt completely dissolved, leaving (*D*) only epoxy.

High concentrations of adsorbed elements such as F, As, heavy metals, and Al are toxic to organisms and plants (9, 25), whereas K, PO_4, N, Fe, and Si are nutrients (11), especially for marine plankton. The XPS surface composition allows us to say that the explosive ash that fell over southern Iceland and that reached Europe, as well as the typical, glassy ash, had hazardous F concentrations. Abundant fluoride on vegetables or in drinking water is of particular concern because high concentrations cause painful bone disorders. Fluoride was clearly associated with significant loss of life during the Laki eruption in the late 1700's, when 50% of Iceland's livestock perished, mainly from fluoride poisoning (34–36).

Implications

The ash from the initial, explosive stage was very fine grained and was ejected more than 9-km high, so it traveled far. The very sharp, hard particles put aircraft at risk from abrasion on windows and body and from melting in jet engines. In the lab, ash particles did not become less sharp during 2 wk of stirring in water, so airborne particles would remain sharp even after days of interaction with each other and water in clouds. Thus, concerns for air transport were well grounded.

Ashfalls in Iceland were certainly hazardous for inhalation and ingestion by grazing animals where particle density was high, but by the time the plume reached Europe, dispersion had significantly decreased density. Although much of the material that reached Europe was <10 μm, thus in the hazardous range, long term exposure to air with concentrations higher than those experienced would be required for a real health risk. About 0.5 mass % of the explosive ash was soluble.

From the results of this study, we can recommend a protocol for rapidly assessing risk from volcanic ash in the future. Size, shape, and hardness are the key parameters for estimating ash abrasiveness, to determine risk for aircraft. BET surface area measurements allow a fast estimate of relative particle size; SEM provides pictures where the range of particle diameter and shape can be observed; and XRD gives mineral composition, from which hardness and melting temperatures can be derived. These techniques are standard and widely available in Earth science laboratories. Together with estimates of the mass of ash produced, plume height, grain size distribution, and the dispersion rate, these data would provide input for modeling to predict the hazard level for aircraft and the transport extent for assessing inhalation risks. For collecting additional parameters, such as those necessary for decisions about chemical toxicity, we recommend standard leaching tests supplemented by XPS surface analysis on fresh, water exposed, and nitric acid exposed samples. XPS is a routine technique in materials science laboratories. Definition of elemental identity and concentration for the salts condensed on ash particles and their relative solubility takes less than a day per sample. These data, with particle size and flux, would allow estimation of toxicity for inhalation and ingestion. The effect of ash on albedo, such as for provoking climate instabilities, and fertilization of the oceans are longer term issues where rapid decisions are not necessary.

Materials and Methods

We collected explosive ash on the ground at 12:30 PM GMT, April 15, 2010, approximately 55 km east of the crater. The ash was approximately 2-mm thick and had fallen during the previous hours. At the time of sampling, the plume was moving north, away from the site. The typical ash was collected about 10 km northwest of the summit crater on a clean plastic sheet (5×21 ft) as it fell from the plume on April 27, from 9:20 AM to 2:30 PM GMT. None of the material had been exposed to fog or rain. Fresh ash is hygroscopic, so samples were analyzed immediately, in some cases within a day or two. Samples were taken from the internal volume of the sample bags, to ensure minimal exposure to humidity. For long-term storage, samples were kept in desiccators.

Polished sections for EMPA were prepared by standard procedures, embedding the ash in epoxy and coating with carbon. SEM samples were examined without conductive coating so they could be returned to experiments for further reaction. For grain size distribution, the >250-μm fraction was sieved and the ≤250-μm fraction was measured using laser absorption in a dry dispersion, created using vibration, differential pressure, and air. The lower detection limit was 1.8 μm.

The leaching experiments were made in open polypropylene beakers where approximately 0.1 g ash was reacted with 100 mL doubly deionized (MilliQ) water that was stirred just enough to put the solid into suspension and then left to settle. Reaction times ranged from 4 to 85 min. Leachate was separated using 0.2 μm cellulose acetate filters. Major and some minor or trace elements were analyzed using ion chromatography (IC) and inductively coupled plasma optical emission spectroscopy (ICP-OES). The leaching procedure was adapted slightly to prepare samples for XPS analysis. Dry ash (50 mg) was mixed with 50 g of either MilliQ water (initial $pH = 5.7 \pm 0.1$), as a model for rain or runoff water, or 10^{-3} M HNO_3 (initial $pH = 3 \pm 0.05$), as a model for acidic volcanic emissions, and placed in 50 mL polypropylene centrifuge tubes. The tubes were constantly agitated on a shaker table (175 rpm) for 90 min, then twice centrifuged (5 min at $4{,}500 \times g$) to remove the supernatant. The remaining solids were dried for a day in a glove box (98% N_2, 2% H_2).

XPS samples were prepared by pressing ash into 3-mm diameter, 2-mm deep cavities on stainless steel stubs and introduced into the analytical chamber when load lock pressure reached approximately 5×10^{-7} Torr. Spectra were collected using monochromated $Al_{K\alpha}$ (1,486.6 eV, 150 W) radiation. The analytical chamber base pressure was 5×10^{-10} Torr and never exceeded 5×10^{-9} Torr during the experiments. The scan procedure was identical for all samples to ensure comparability and no evidence of beam damage could be found. Data were treated with commercial software, CasaXPS, using Shirley background correction.

AFM and AFS data were collected using an Asylum MFP3D optimized for force/volume analysis. We used DanLim 334 epoxy cured for 24 h, for attaching the single ash particles to standard silicon cantilevers. Picogram mass-loss experiments are very tricky; we made about 10 experiments to ensure reproducibility.

ACKNOWLEDGMENTS. Thanks to Matthias Schroter, Max Planck Göttingen for tomography; Keld West and Kim Dalby, NanoGeoScience, Copenhagen, for BET analyses; Helene Almind, Alfons Berger, Hector Diaz, Klaus Qvortrup, Nicole MacDonald, and Andrew Burrows for help and access to equipment; Domenik Wolff-Boenisch, Snorri Gudbrandsson, Ármann Höskuldsson, and Reynir Ragnarsson from the Iceland team for technical help; and Bob Berner and two anonymous reviewers. Funding was provided by the Icelandic Government and the Institute of Earth Sciences, Reykjavik, and the NanoGeoScience laboratory was founded with a grant from the Danish National Research Council.

1. Gudmundsson MT, et al. (2010) Eruptions of Eyjafjallajökull volcano. *Eos* 91:190–191.
2. Moody E (2004) Gliding a B747 out of volcanic ash. *Proceedings of the Second International Conference on Volcanic Ash and Aviation Safety, June 21–24, 2004* (Office of the Federal Coordinator for Meteorological Services and Supporting Research, Silver Spring, MD).
3. Horwell CJ, Baxter PJ (2006) The respiratory health hazards of volcanic ash: A review for volcanic risk mitigation. *Bull Volcanol* 69:1–24.
4. Fubini B, Fenoglio I (2007) Toxic potential of mineral dusts. *Elements* 3:407–414.
5. Baxter PJ, et al. (1999) Cristobalite in volcanic ash of the Soufriere Hills Volcano, Montserrat, British West Indies. *Science* 283:1142–1145.
6. Cronin SJ, Hedley MJ, Neall VE, Smith RG (1998) Agronomic impact of tephra fallout from the 1995 and 1996 Ruapehu volcano eruptions, New Zealand. *Environ Geol* 34:21–30.
7. Cronin SJ, Neall VE, Lecointre JA, Hedley MJ, Loganathan P (2003) Environmental hazards of fluoride in volcanic ash: A case study from Ruapehu volcano, New Zealand. *J Volcanol Geotherm Res* 121:271–291.
8. Mather T, Pyle DM, Oppenheimer C (2003) *Volcanism and the Earth's Atmosphere*, eds A Robock and C Oppenheimer (Am Geophysical Union, Washington, DC), pp 189–212.
9. Kockum PCF, Herbert RB, Gislason SR (2006) A diverse ecosystem response to volcanic aerosols. *Chem Geol* 231:57–66.
10. Flaathen TK, Gislason SR (2007) The effect of volcanic eruptions on the chemistry of surface waters: The 1991 and 2000 eruptions of Mt. Hekla, Iceland. *J Volcanol Geotherm Res* 164:293–316.
11. Jones MT, Gislason SR (2008) Rapid releases of metal salts and nutrients following the deposition of volcanic ash into aqueous environments. *Geochim Cosmochim Acta* 72:3661–3680.
12. Brunauer S, Emmett PH, Teller E (1938) Adsorption of gases in multimolecular layers. *J Am Chem Soc* 60:309–319.
13. Wolff-Boenisch D, Gislason SR, Oelkers EH, Putnis CV (2004) The dissolution rates of natural glasses as a function of their composition at pH 4 and 10.6, and temperatures from 25 to 74 degrees C. *Geochim Cosmochim Acta* 68:4843–4858.
14. Delmelle P, Villieras F, Pelletier M (2005) Surface area, porosity and water adsorption properties of fine volcanic ash particles. *Bull Volcanol* 67:160–169.
15. Riley CM, Rose WI, Bluth GJS (2003) Quantitative shape measurements of distal volcanic ash. *J Geophys Res* 108:2504.
16. Baxter PJ (2005) *Volcanoes and the Environment*, eds J Marti and GG Ernst (Cambridge Univ Press, Cambridge, UK), pp 273–303.
17. Bursik MI, Sparks RSJ, Gilbert JS, Carey SN (1992) Sedimentation of tephra by volcanic plumes. 1. Theory and its comparison with a study of the Fogo-A plinian deposit, So-miguel (Azores). *Bull Volcanol* 54:329–344.
18. Durant A, Bonadonna C, Horwell CJ (2010) Atmospheric and environmental impacts of volcanic particulates. *Elements* 6:235–240.
19. Ghiorso MS, Sack RO (1995) Chemical mass transfer in magmatic processes. IV. A revised and internally consistent thermodynamic model for the interpolation and extrapolation of liquid-solid equilibria in magmatic systems at elevated temperatures and pressures. *Contrib Mineral Petrol* 119:197–212.
20. Hünecke K (1997) *Fundamentals of Theory, Design and Operation* (Airlife, Shrewsbury, UK) p 241.
21. Soares C (2007) *Gas Turbines: A Handbook of Air, Land and Sea Application* (Butterworth-Heinemann, Oxford) p 776.
22. Witham CS, Oppenheimer C, Horwell CJ (2005) Volcanic ash-leachates: A review and recommendations for sampling methods. *J Volcanol Geotherm Res* 141:299–326.
23. Stipp SL, Hochella MF (1991) Structure and bonding enviroments at the calcite surface as observed with X-ray photoelectron-spectroscopy (XPS) and low energy diffraction (LEED). *Geochim Cosmochim Acta* 55:1723–1736.
24. Oelkers EH, Gislason SR (2001) The mechanism, rates and consequences of basaltic glass dissolution: I. An experimental study of the dissolution rates of basaltic glass as a function of aqueous Al, Si and oxalic acid concentration at 25 degrees C and pH = 3 and 11. *Geochim Cosmochim Acta* 65:3671–3681.
25. Frogner P, Gislason SR, Oskarsson N (2001) Fertilizing potential of volcanic ash in ocean surface water. *Geology* 29:487–490.
26. Parkhurst DL, Appelo CAJ (1999) User's guide to PHREEQC (Ver. 2). *A Computer Program for Speciation, Batch-Reaction, One-Dimensional Transport, and Inverse Geochemical Calculations, US Geol Surv Water Resour Invest Rep* 99-4259.
27. Alkattan M, Oelkers EH, Dandurand JL, Schott J (1997) Experimental studies of halite dissolution kinetics. 1. The effect of saturation state and the presence of trace metals. *Chem Geol* 137:201–219.
28. Raines MA, Dewers TA (1997) Mixed transport reaction control of gypsum dissolution kinetics in aqueous solutions and initiation of gypsum karst. *Chem Geol* 140:29–48.
29. Gislason SR, Oelkers EH (2003) Mechanism, rates, and consequences of basaltic glass dissolution: II. An experimental study of the dissolution rates of basaltic glass as a function of pH and temperature. *Geochim Cosmochim Acta* 67:3817–3832.
30. Pokrovsky OS, Schott J (2000) Kinetics and mechanism of forsterite dissolution at 25 degrees C and pH from 1 to 12. *Geochim Cosmochim Acta* 64:3313–3325.
31. Wolff-Boenisch D, Gislason SR, Oelkers EH (2004) The effect of fluoride on the dissolution rates of natural glasses at pH 4 and 25 degrees C. *Geochim Cosmochim Acta* 68:4571–4582.
32. Stoiber RE, Rose WI (1974) Fumarole incrustations at active Central American volcanoes. *Geochim Cosmochim Acta* 38:495–516.
33. Doner HE, Lynn WC (1989) *Minerals in Soil Enviroments*, eds JB Dixon and SB Weed (Soil Science Soc of Am, Madison, WI), 2nd Ed,, pp 331–378.
34. Thorarinsson S (1969) The Lakagigar eruption of 1783. *Bull Volcanol* 33:910–929.
35. Grattan JP, Charman DJ (1994) Non-climatic factors and the environmental impact of volcanic volatiles: Implications of the Laki Fissure eruption of AD 1783. *Holocene* 4:101–106.
36. Steingrimsson J, Kunz K (1998) *Fires of the Earth, The Laki eruption 1783–1784* (Univ of Iceland Press, Reykjavik, Iceland) p 96.
37. Hassenkam T, Skovbjerg LL, Stipp SLS (2009) Probing the intrinsically oil-wet surfaces of pores in North Sea chalk at subpore resolution. *Proc Natl Acad Sci USA* 106:6071–6076.